

# An experimental and numerical study of steel tower response to blast loading

J.D. Baum, O.A. Soto, and C. Charman

*Center for Applied Computational Sciences, Special Projects Division SAIC,  
1710 SAIC Drive, MS 2-6-9, McLean, VA 22102 (USA)*

## 1 Introduction

Over the last several years we have developed and applied a coupled CFD and CSD methodology for modeling blast wave interaction with structures and the structural response to the blast loading. One of the more interesting and more complex simulations conducted was a simulation of a terrorist attack on a generic steel tower that supports a suspension bridge, modeled as a multi-chamber, multi-floor bridge-support steel tower. The numerical methodology models the HE detonation initiation, the detonation wave propagation within the explosive, detonation products diffraction after detonation completion, blast load interaction with the structure, structural deformation, steel panel fragmentation and blast load diffraction between the accelerating fragments to load the next layer of steel panels (cells). The results demonstrated that structural failure could result from either large pressure loading or high-velocity fragment impact. To validate the results, the University of California, San Diego (UCSD) and Energetic Material Research and Testing Center (EMRTC) of New Mexico Tech (NUMTECH) initiated a test program, under TSWG sponsorship, that tested scaled sections of a steel-tower to blast loading. Simultaneously, SAIC conducted a sequence of numerical simulations of this event. The paper presents the experimental results and the numerical predictions, while concentrating on the analysis of the predictions. It is concluded that the simulations raised some serious issues, which require further precision testing.

## 2 The Numerical Methodology

Mesh generation for both CSD and CFD models is performed using FRGEN3D [3], which is based on the advancing front method. The CFD mesh is composed of triangular (surface) and tetrahedral (volume) elements. The CSD mesh includes beams, triangular or quad shells and bricks for the solids. The flow solver employed is FEFLO98, a 3-D adaptive, unstructured, edge-based hydro-solver based on the Finite-Element Method Flux-Corrected Transport (FEM-FCT) concept [4]. It solves the Arbitrary Lagrangean-Eulerian (ALE) formulation of the Euler and Reynolds-averaged turbulent, Navier-Stokes equations. The high order scheme used is the consistent-mass Taylor-Galerkin algorithm. Combined with a modified second-order Lapidus artificial viscosity scheme, the resulting scheme is second-order accurate in space, and fourth-order accurate in phase. Other high-order accuracy shock capturing schemes, such as HLLC, WENO, HWENO, etc, are available, and can be used for specific applications. The spatial mesh adaptation is based on local H-refinement, where the refinement/deletion criterion is a modified H2-seminorm [4] based on a user-specified unknown. Most of the shock wave propagation cases require

the use of a blend of density and energy. FEFLO98 supports various equations of states including real air, water, SESAME and JWL with afterburning. The structural dynamics solver are either GA-DYNA3D [5] or SAICSD [8], both are unstructured, explicit finite element codes, well suited for modeling large deformations and provide good base for non-linear materials with elasto-plastic compartmental laws with rupture. Both codes incorporate a large library of materials and various equations-of-state, as well as many kinematic options, such as slidelines and contacts. The structural failure is described using the Johnson and Cook nonlinear plastic hardening function [1] that contains strain rate effects in both the yield and damage functions. The yield stress is a nonlinear function of the effective plastic strain, augmented by a strain rate term which increases the yield strength with increasing strain rate, and a thermal softening term which lowers the yield strength with increasing temperature. Heat is generated in the model by plastic work, and the resulting temperature rise is computed using the specific heat for the material assuming adiabatic conditions. The Johnson and Cook (J&C) model defines the failure strain as a function of the ratio of the pressure stress to the effective stress, strain rate, and temperature [Eq. 81 of the Dyna3D Manual [2]]. The material damage is computed by summation of the plastic strain increments divided by the strain to failure over each time step. Because of the term involving the ratio of pressure stress to the effective stress, the failure strain is large in compressed regions of the model, though little damage will occur in theses compressed regions. When this damage is greater than 1.0, the element is assumed to have failed and is eliminated from the calculation by an erosion algorithm. If the eroded element has any face exposed to the blast pressure, new pressure surfaces are determined and given back to the flow code to evaluate the new external surface of the model and to determine the pressures for the next structural step for the coupled CSD/CFD simulation. In these simulations we are using 60% of the true strain to failure when we evaluate the damage in an element. This is based on engineering judgment and correlation with earlier experiments, adjusted up to account for finer mesh resolution at the failure areas.



**Fig. 1.** Test especiment before and after the test

### 3 The Experimental Facility and Results

A field test was conducted at EMRTC to investigate the response of a single row of cells to an explosive load, simulating the response of a full scale section of a typical steel cellular bridge tower to blast loading. The specimen consisted of three cells each 3-6 tall by 3-6 wide and 8-0 in length, constructed of 7/8 A36 steel plates and connected at the

intersections via 8 x 8 x angles and 1 diameter A307 bolts at 4 on center. The specimen was loaded with 220 lbs of flake TNT with a C4 detonator with approximately 6 of stand-off at the midspan of the center cell. The results show a flyer plate of approximately the same dimensions as the charge was created in the top plate of the center cell directly below the applied load. The 2 square impacted the bottom steel plate of the test specimen, creating a second flyer plate. The speed of the first flyer plate before impact with the bottom plate was approximately 3,400 feet per second. In addition to the holes left by the separation of the flyer plates, the test specimens showed significant deformation: the edges of the hole in the top plate showed substantial petalling and tearing of the steel plate. The rupture of the top plate occurred in the center cell where the explosive load was placed. In addition, the bolts and the angle that supported the plates also deformed. The angle pieces stayed connected to the sidewalls of the center cell but the supporting leg was bent. The steel section seen in front of the specimen is what remains of the top plate where it came to rest after the second test. Figure 1 shows the test specimen before (Fig. 1a) and after (Fig. 1b) the test. Figure 1c shows an expanded view of the bottom plate, while Fig 1d shows the two flyer plates. The indentation in the flyer plates was caused by the impact of the charge downwards. The destruction caused by the flyer plates and the plate in the foundation can be seen in Fig 1b. A variety of failure modes were seen in the bottom plate. The bottom plate also deformed before shearing. In addition to the deformation of the plate due to the projectile, one can also see the tearing of the angles and the loss of the connections to the bottom plate. The plate is actually resting on the foundation and is no longer connected to the support angles by bolts.

## 4 Numerical Results

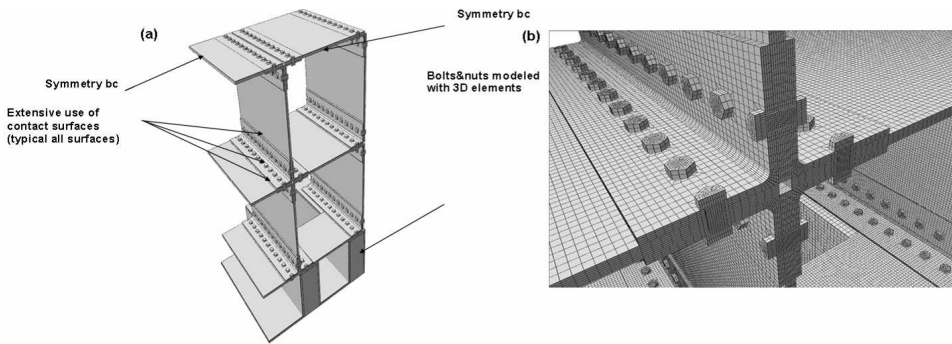


**Fig. 2.** Numerical model and details of a typical bolted joint

**The CSD Model:** The model includes only a quarter of the test facility, taking advantage of the double symmetry. The material model used employed the Johnsons and Cook plasticity model, where the A-36 steel parameters were taken of [6]. The A307 bolts were modeled with the same hardening parameters, but with a fracture strain of 18%. The concrete was modeled as rigid. Fracture represented by erosion of elements with damage parameter  $>1$ . Contact conditions were used between all parts. The quarter-symmetry CSD model used in the simulations is shown in Figs 2. Figure 2a shows the set-up. The

explosive is set on top, with a standoff distance of six inches. The solid elements were sized 0.4X0.5X0.125 inches for the angles and plates, and 0.125X0.125X0.125 inches for the bolts. The resulting CSD mesh included 868,724 hex elements, 1,094,683 nodal points, 58 contact conditions and 431,482 wet faces to obtain pressure data from the flow solver. Results: The first simulation modeled the structure as plates (shells). As the plate model did not adequately capture the interaction between the bolts, nuts, angles and plates at the connections, it was felt that a 3-D model (solids) would better represent the physics. This model can better represent the complex stress states and produce necking as well as model all six components of the stress. The next issue arose with the failure algorithm. The J&C material model uses true stress true strain (Cauchy stress logarithmic strain). However, deformation can localize in material forming necking at the fracture location. This produced significant mesh sensitivity. The material failure model (ultimate strain value) was adjusted to account for the size of the element relative to gage length and wide variation in response was noted using above approach. To further investigate mesh effect we conducted a sensitivity study that included three plates 6 inch apart. Mesh sizes tested were 1/16, 1/8 and 1/4 inch. The solutions from 1/8 and 1/16 are almost identical, hence the multi-cell models were reworked to include 1/8 inch zone in area where tearing was observed in experiment. The simulation modeled 220 lbs of flake TNT, with a C4 detonator. The charge was placed six inches of standoff at the midspan of the center cell. As no EOS exists (to our knowledge) for flake TNT (flake TNT is usually melted and cast), we conducted several simulations varying the TNT equivalence of the flake TNT. Rough estimate shows that it's TNT equivalence is about 0.25 to 0.3. Naturally, for precision testing and code validation, we require a more precise source definition. The time evolution of the detonation wave propagation in the explosive, and the resulting blast wave evolution are fairly straight forward: charge detonation followed by detonation product diffraction and load on the top surface, followed by top surface failure and blast wave propagation through the cracking steel surface. These are depicted in Figures 3a through 3h. The choice of ultimate strain of 0.6 allows large deformation before plate cracking (Fig 3b) and break-up (Figs 3c and 3d). The resulting flyer plate is strongly deformed (Fig 3e). Similar processes are observed as the flyer plate impacts the second plate, to form a second flyer plate, i.e., significant deformation before plate cracking and formation of a second flyer plate (Figs 3f and 3g). To further investigate the role of the critical effective plastic strain (the ultimate strain value) on energy absorption, flyer plate shape and speed, we varied the ultimate strain value from 0.2 to 0.6. The more brittle material formed a flyer plate with very little deformation. As significantly less energy was spent on plastic work, the flyer plate has a higher velocity and higher kinetic energy, and is capable of penetrating more layers in the adjacent cells than the slower deformed flyer plate (for ultimate strain of 0.6). Another difference between the brittle and ductile materials: for the higher ultimate strain values, the two (or three) flyer plates fly together, while for the brittle materials, the transfer of kinetic energy is almost perfectly, and the impacting plate transferred all of it's kinetic energy to the newly formed flyer plate (Fig 4a). In yet another study we defined the ultimate strain for the top plate as 0.2, and for the second plate as 0.4. Figure 4b shows the top flyer plate to be fairly flat (typical of a brittle material), while the second plate (the more ductile material) deformed significantly before the effective plastic strain surpassed it's ultimate strain value, and the plate broke-off. Comparison of the final status obtained with ultimate strain values of 0.2, 0.4 and 0.6 (0.2 and 0.6 are shown in Figs 3h and 4a, respectively), to the experimental results (Figs 1b to 1d) shows very good reproduction

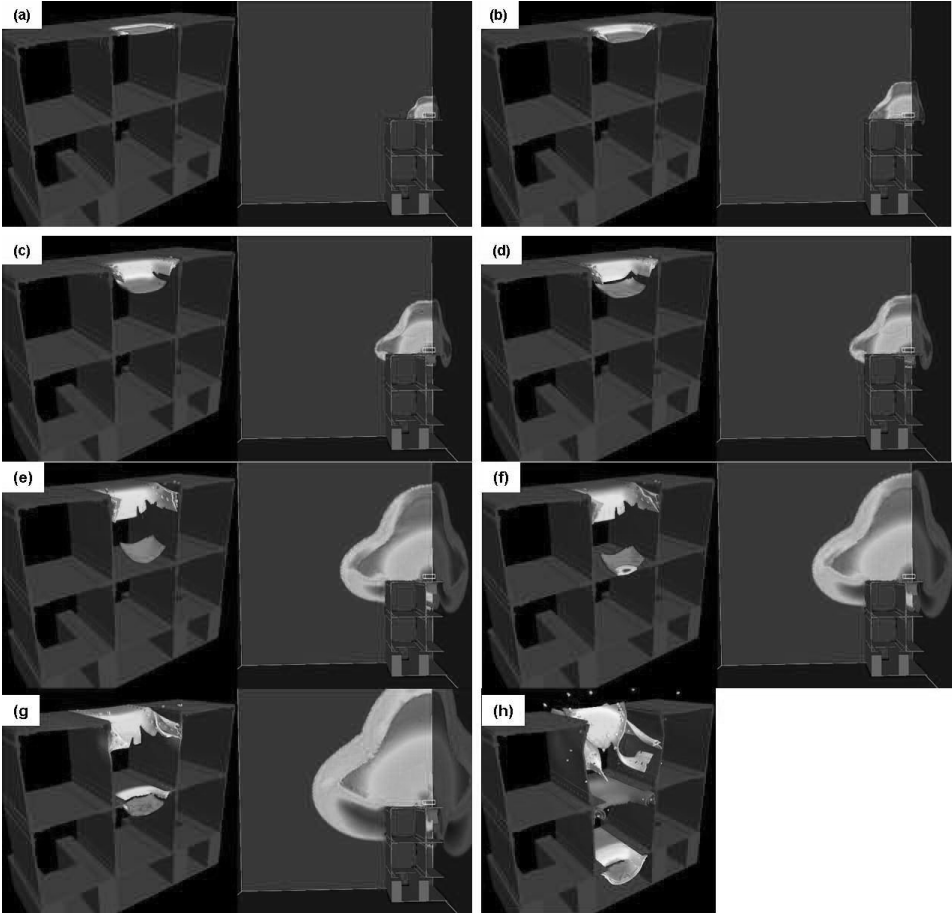


Fig. 3. Evolution of the blast and structural response

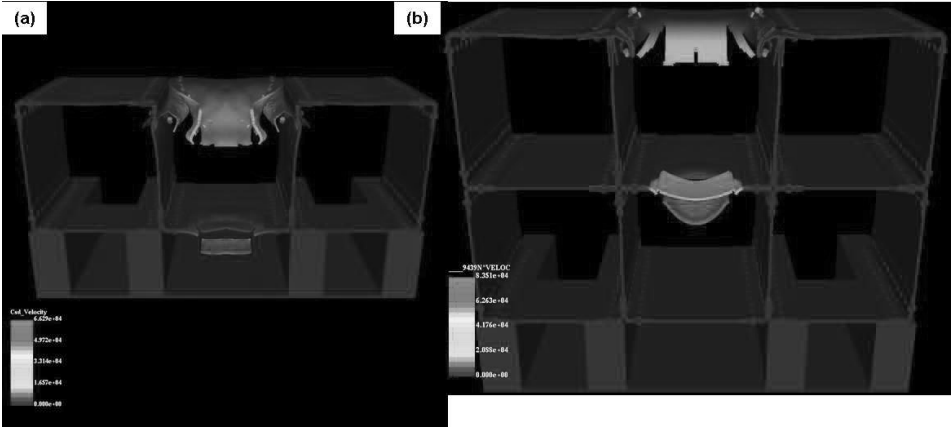


Fig. 4. Evolution of the blast and structural response

of most the deformations discussed above. The size and cut of the predicted flyer plates were almost identical to the experimental one (basically, the explosive box imprint). Both the curvature and speed of the flyer plate best agreed with the results obtained with an ultimate strain value of 0.4. However, these results are inconclusive due to the uncertainty about the source. The results show that determination of the ultimate strain value is critical to modeling the flyer plate shape and speed, and hence the collateral damage inflicted by the charge (i.e., damage to next layer cells). In the next sequence of tests we will use well-characterized ideal explosives, eliminating the issue of an ill-defined source. These should help define the ultimate strain. Following these tests, we will be able to confidently predict the complete tower response to an explosive charge.

## 5 Conclusions

This paper describes a numerical and experimental investigation directed at improved understanding and modeling of the vulnerability of steel towers to terrorist attacks using bare HE charges. Large scale numerical simulations gave indicated the possible vulnerability of large steel towers to terrorist attacks. As testing of these tower is impractical, it became necessary to validate the predictions against scaled tests. We conducted numerical predictions and experiments under which scaled cells of the steel tower were exposed to blast loading. While the numerical predictions were capable of simulating the damage observed in the experiments, it was impossible to fully validate the predictions, as the explosive used does not have a fully validated equation-of-state. Future tests will be conducted with more cells and with a commonly used ideal explosive (such as C-4, Comp-B, etc.), to eliminate any uncertainty about the source strength.

## References

1. Johnson, G.R. and W.H. Cook, A Constitutive Model and Data for Metals Subjected to Large Strains, High Strain Rates and High Temperatures, Presented at the Seventh International Symposium on Ballistics, the Hague, The Netherlands, April. 1983.
2. Lin, J.I., DYNA3D A Nonlinear, Explicit, Three-Dimensional Finite Element Code For Solid and Structural Mechanics- User Manual, Lawrence Livermore National Laboratory, UCRL-MA-107254, January, 1995.
3. R. Löhner and P. Parikh - Three-Dimensional Grid Generation by the Advancing Front Method; *Int. J. Num. Meth. Fluids* 8. 1135-1149(1988).
4. R. Löhner and J.D. Baum - Adaptive H-Refinement on 3-D Unstructured Grids for Transient Problems; *Int. J. Num. Meth. Fluids* 14, 1407-1419 (1992).
5. D. Pelessone and C.M. Charman - A General Formulation of a Contact Algorithm with Node/Face and Edge/Edge Contacts; 1998 ASME Pressure Vessels and Piping Conference, San Diego, Ca, July (1998).
6. Seidt, J.D., Constitutive and Fracture Models for ASTM A36 Hot Rolled Steel, Battelle, Columbus, Ohio, November 2005 (Draft)
7. Optional Strain-Rate Forms for MAT\_JOHNSON\_Cook and the Role of the Parameter, Len Schwer, March2006, DRAFT
8. O. Soto, Baum, J. Löhner, R., and Mestreau, E. An Efficient CSD FE Scheme for Blast Simulations, presented at the 2007 Coupled Problems Conference, May 21-23, Ibiza, Spain.

Shock Waves

26th International Symposium on Shock Waves, Volume  
2

Hannemann, K.; Seiler, F. (Eds.)

2009, XXX, 774 p.,

ISBN: 978-3-540-85181-3